121

LIFE-TESTING OF 1.7 kW h ZINC–CHLORIDE BATTERY SYSTEM: CYCLES 1 - 1000

C. M. BLEVINS

Battery Research and Development, Energy Development Associates, 1100 W. Whitcomb Avenue, Madison Heights, MI 48071 (U.S.A.)

Summary

A 1.7 kW h battery system was built and tested in 1976 as one part of a program to develop the zinc–chloride battery for utility load-leveling. The two volt, multiple-cell battery stack is of particular interest because it embodies many of the design concepts utilized in the present technology at Energy Development Associates (EDA) for both electric vehicle and load-leveling applications, *e.g.*, porous graphite–chlorine electrodes. From early 1977 onwards, cycle-testing of the system was conducted with a data acquisition and control system (DACS). As of June 1979, the system accumulated 1000 charge–discharge cycles. As indicated by the constancy of the voltaic efficiency, the performance deterioration through 1000 cycles was negligible. EDA plans to continue testing through 2500 cycles — the life target for the commercial version of the load-leveling battery.

Introduction

Energy Development Associates is currently developing a zinc–chloride battery system for utility load-leveling and electric vehicle applications. During the early development of the battery, a number of test batteries were designed and cycled to test the feasibility of the battery system. The first, built in mid-1974, was a 1 kW h battery with the chlorine electrodes made of ruthenia-catalyzed titanium. The second design, rated at 1.4 kW h, was an upgraded version of the 1 kW h battery. It was put on test in early 1976. Concurrently, a 1.7 kW h battery, which employed porous graphite–chlorine electrodes, was assembled and put on test. The 1.4 kW h titanium-electrode system was retired in late 1977 for a number of reasons: performance sensitivity to changes in pH, a relatively low overpotential for hydrogen formation, and its higher material cost [1]. Life testing of the 1.7 kW h system, which is shown in Fig. 1, has continued since 1976 and in June 1979 it completed 1000 charge/discharge cycles. This two volt, multiple-cell battery will hereafter be referred to as a cell system to avoid confusing it with a full-scale 50 kW h battery module.
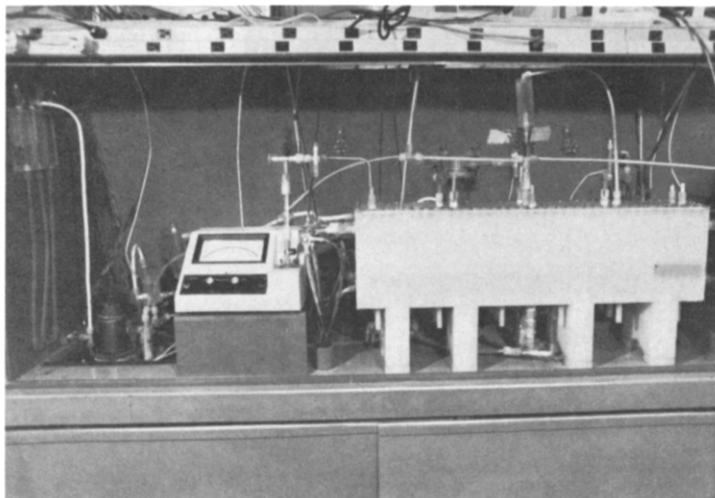
Fig. 1. Photograph of 1.7 kW h zinc–chloride system installed in laboratory hood.

Although the 1.7 kW h system was designed for the load-leveling application, the cell materials are similar to those used in the electric vehicle application. Therefore, data and results obtained from the program are applicable to both. The major differences in the two applications are the electrolyte formulation and the media for forming chlorine hydrate, which is water for the Load Leveler™ unit and electrolyte for the electric vehicle battery (Electric Engine™). In addition, there are variations in the primary objectives of the two applications: power and energy densities for the electric vehicle battery in contrast to efficiency and cost/kW h for the Load Leveler™ unit.

Because the porous graphite–chlorine electrode material is considered to be the life-limiting component of the battery, the 1.7 kW h test system has been operated continuously to demonstrate the stability of the electrodes over the targeted cycle life of a commercial load-leveling system: 2500 cycles consisting of 1 cycle/day, 5 days/week, 50 weeks/year for 10 years. Initially, there was concern over electrode life because graphite anodes in chlor-alkali cells are known to demonstrate a limited life, i.e., less than one year. However, differences in the operational parameters of the 1.7 kW h system — specifically the acidity — are theorized to aid in prolonging electrode longevity [2] and, therefore, the targeted life of the zinc–chloride system. A secondary goal of this test program is to demonstrate that zinc–chloride systems can operate for extended periods with no electrolyte maintenance.

System description

Although the 1.7 kW h cell was built in early 1976, several components in the stack represent current state-of-the-art technology. These components

are the dense graphite–zinc electrode substrates, the porous graphite–chlorine electrode substrates, the dense graphite buses, and the interference fit between the electrode substrates and the bus.

The 1.7 kW h system is a breadboard system. However, it contains all of the subsystems, *e.g.*, a stack and a separate store, found in a zinc–chloride battery. The stack is the site of the electrochemical reactions. As shown in Fig. 2, the stack is contained in two trays that are enclosed by the outer case.
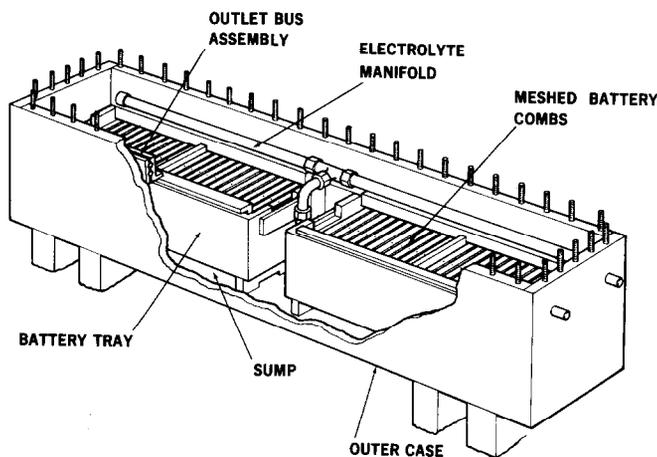
Fig. 2. Cutaway drawing of the 1.7 kW h stack unit. Outer case serves as electrolyte sump and defines major gas space in system. Outer case cover not shown.

The outer case forms the electrolyte sump at the bottom and defines the system's major gas space at the top. Each of the two trays contains one-half of the 96-cell stack. The 48 cells in each tray are made up of 48 chlorine electrode substrates in 24 two-electrode packs and 25 zinc electrode substrates. As illustrated in Fig. 3, the inactive faces of the chlorine electrodes are mated in pairs to form a cavity for the distribution of the electrolyte to the active faces of the cells. The total area of the chlorine electrodes is 6194 square centimeters. Twenty-three of the zinc substrates are active on both sides, while the two electrodes at either end of the cell assembly are active only on the inside face. The interelectrode cell gap is 3 mm.

Electrolyte flows from the sump into the manifold, through the pairs of chlorine electrodes, and past the zinc electrodes. It then overflows the stack area and falls back by gravity into the sump. This flow pattern allows the liberation of a constant supply of zinc and chlorine from the electrolyte for the electrochemical reaction in the stack area during charge, and it introduces the chlorinated electrolyte during discharge to permit the electrochemical recombination of the two elements. Figure 4 is a photograph of a section of the stack area that shows the chlorine electrode pairs, with gas vents to prevent gas locking, and the zinc electrodes.
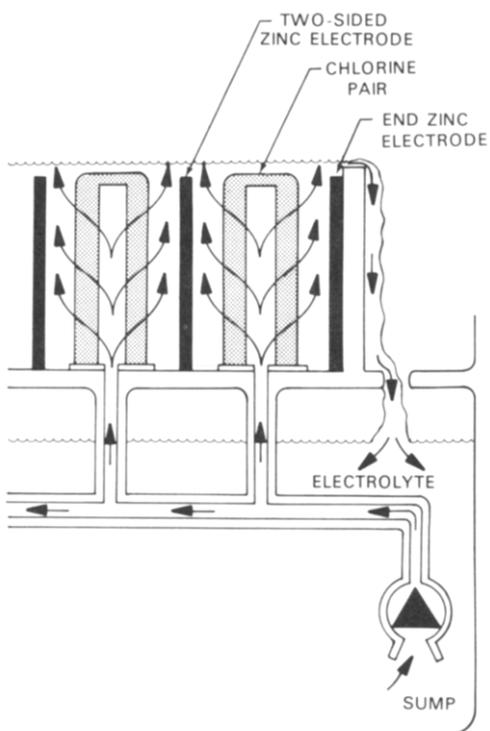
Fig. 3. Schematic representation of chlorine electrode pair and zinc electrode showing electrolyte flow path.
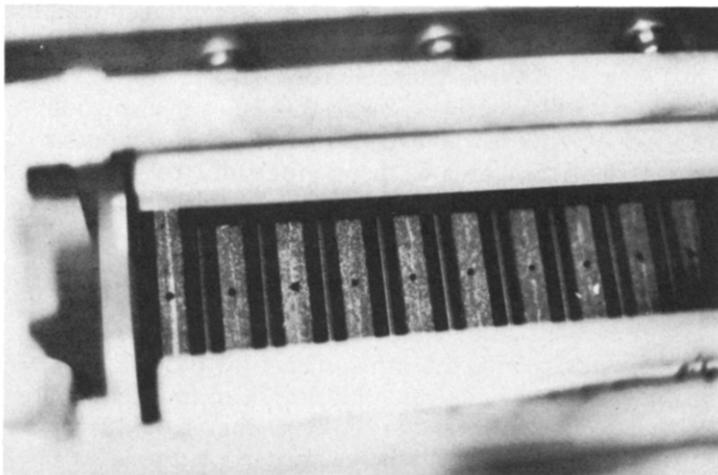
Fig. 4. Photograph of a section of the 1.7 kW h stack area showing zinc and chlorine electrodes. Note vent holes in chlorine electrode pairs.

The operation of the 1.7 kW h system is contingent upon a network of peripheral components that comprise four subsystems. The entire system is illustrated schematically in Fig. 5, including the loops formed by the subsystems. These include the electrolyte loop, the chlorine gas loop, the hydrogen recombination loop, and the hydrate storage and decomposition loop. While the loops will be described in the following sections, a more complete description of them is available elsewhere [3].
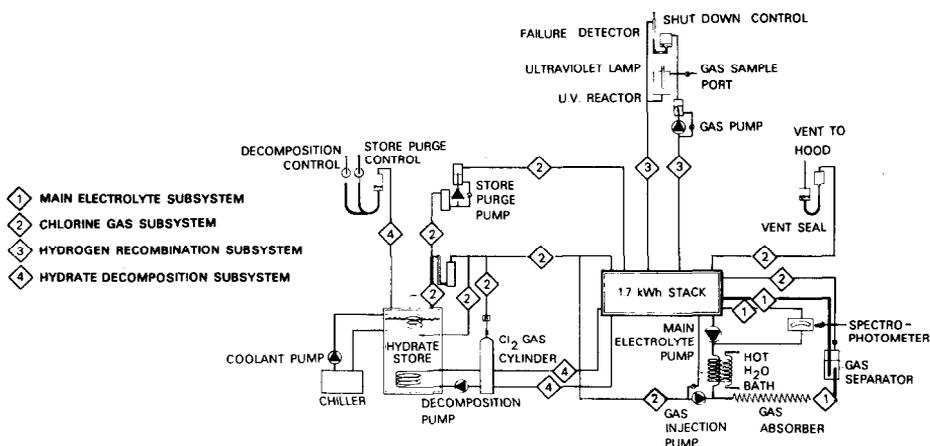
Fig. 5. Schematic diagram of the 1.7 kW h cell system with four numbered subsystems.

(a) Electrolyte subsystem, Loop 1

The main electrolyte loop begins at the bottom of the case where the electrolyte is pumped from the sump through a heat exchanger to maintain constant electrolyte temperature and, during discharge only, chlorine gas is injected into the stream by a micropump. The flow then enters a gas absorber to chlorinate the electrolyte and passes through a gas separator that removes the excess chlorine, after which the electrolyte returns to the stack gas space. The chlorinated electrolyte re-enters the case directly through a manifold. A small amount of electrolyte is continuously pumped through a spectrophotometer that measures the chlorine concentration. The electrolyte capacity required to maintain the desired range of zinc molarity for a 5 h charge is 15 liters.

(b) Gas subsystem, Loop 2

Only one gas line interconnects the store and the stack. During charge, gas exits at the top of the stack and, directed by a differential manometer, flows into the store *via* the inlet tube located below liquid level. On discharge, chlorine evolved from the decomposition of chlorine hydrate passes through the upper exit tube, through the differential manometer, and back into the stack gas space where it is transferred to the gas absorber by the gas

injection pump. A second differential manometer is connected to the gas space area of the stack to prevent excessive pressure on the stack case. The total gas volume of the stack-sump case is 18 liters.

(c) Hydrogen recombination subsystem, Loop 3

The gas recirculation loop exits the case from the gas space and enters a micropump that pumps the gas at a rate of 10 l/min through a chamber containing two ultraviolet lights. These lights catalyze the recombination of chlorine with any free hydrogen evolved from the zinc electrodes.

(d) Hydrate storage and decomposition subsystem, Loop 4

During charge, chlorine and water are combined to form chlorine hydrate in the store. It is formed by pumping cooled ethylene glycol through the store heat exchanger to cool the store water to 5 °C, the temperature at which hydrate readily forms. The chlorine gas enters the store *via* a heated inlet tube above an agitator that mixes the water and chlorine. The precipitated hydrate settles to the bottom of the store as it is formed. On discharge, warm electrolyte from the sump is circulated through a heat exchanger coil in the bottom of the store by a micropump to decompose the hydrate. The decomposition pump is activated during discharge when the store pressure is low.

System operation

Based on projected cycling requirements for a load-leveling battery, a cycling regime was established that consists of the following phases:
- cooldown
- charge
- turnaround
- discharge
- cleanout
- stand.

The cooldown phase (30 min) precedes the charge phase (5 h) in order to chill the store in preparation for chlorine storage. In the turnaround phase (6 min), the cell stands for a short period of time with the gas injection and main electrolyte pumps running to chlorinate the system prior to discharge. The discharge phase begins with a constant current of 190 A, which is maintained until the voltage drops below 1.7. At that time, the current is decreased in 20 A steps to 10 A in order to maintain a minimum voltage of 1.7. Discharge is terminated when the voltage at 10 A drops below 1.7. Total time for the discharge phase is 5.4 h. The cell system is short-circuited in the cleanout phase (45 min) to strip any plated zinc remaining on the zinc electrode substrates. Figure 6 shows a voltage–time trace for a typical cycle. Since the onset of testing the 1.7 kW h system in early 1976, the cycling regime has been conducted using the test conditions shown in Table 1. These
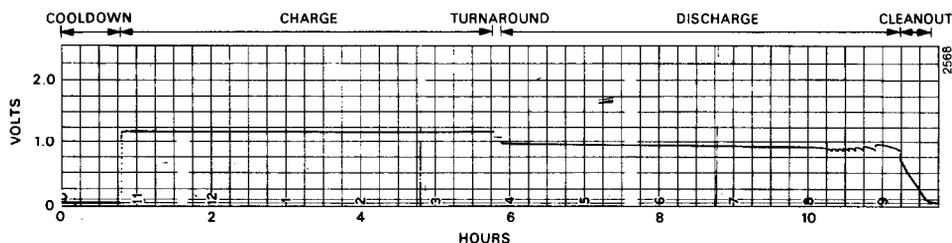
Fig. 6. Voltage–time trace for a typical cycle of the 1.7 kW h cell system.

TABLE 1

1.7 kW h system test conditions

	Charge	Discharge
Current (A)	220	190
Current density (mA/cm^2)	35.5	30.8
[Cl$_2$] (g/l)	1.3	1.3
Temp. (°C)	40	40
Pressure	ambient	ambient

conditions continue to be employed in order to maintain a consistent data base of test results. A stand phase was established to simulate the anticipated conditions of commercial load-leveling battery systems, which will most likely stand for extended periods of time (up to 12 h/d) between the end of one cycle and the beginning of another.

Data acquisition and control system

The 1.7 kW h cell system was cycled manually for almost one year until early 1977 when a data acquisition and control system (DACS) was installed. The manual cycling regime was conducted for 8 - 10 h/day, 5 days/week. Under automatic control, the system was expected to cycle 24 h a day, 7 days a week with a minimum of human intervention. Thus, in order to maintain a consistent data base, the controller was programmed to continue cycling in the mode established under manual control. It also had to provide for any contingencies that might arise when it was unattended. A major concern was the failure of components or subsystems that could cause damage to the cell itself.

In addition to failure detection capabilities, the automatic controller was programmed to record data on performance parameters every five minutes. Under manual control, data on such parameters as current and voltage were recorded once each hour. Other advantages of the DACS include a visual display and the ability to reduce and manipulate data.

The data acquisition system consists of a standard 19 in. relay rack containing a microprocessor, a cathode ray tube (CRT) for data display, and

all interfacing between the cell system and its components. A computer terminal also is included in the data acquisition system to retrieve data as hard copy for instant use and to record data on cassette tapes for insertion later into a data base [4]. The tasks of this system are cycling and auxiliary subsystem control; monitoring of operating parameters; collection and display of data; detection of and response to failures; and reduction of time, current, and voltage to amp-hours, watt-hours, and efficiencies.

Test results

Figure 7 is a plot of efficiency as a function of cycle number for the 1000 accumulated cycles. The performance parameter of greatest interest in this program is voltaic efficiency because it can indicate degradation of the chlorine electrodes. As can be seen, over the duration of cycles there has been an apparent decline in voltaic efficiency of 1%. Secondly, there is a reciprocal relationship between the coulombic and voltaic efficiencies. This occurs because conditions that optimize one of them tend to decrease the other in the zinc–chloride battery.

As shown in the Figure, a slight loss in electrochemical energy efficiency has occurred over the period of 1000 cycles. Bivariate linear regressions were run comparing electrochemical energy efficiency with the voltaic and coulombic efficiencies in an attempt to correlate this 2% loss (from 65 to 63). It was found that there was a greater correlation between energy efficiency and coulombic efficiency than there was with voltaic efficiency. Therefore, it is felt that most of the losses in energy efficiency (ϵ_e) were due to coulombic efficiency (ϵ_c) losses rather than voltaic efficiency (ϵ_v) losses.
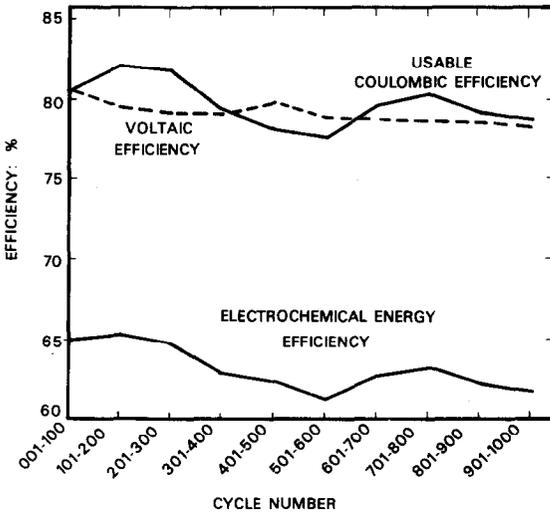
Fig. 7. Performance efficiencies of the 1.7 kW h system plotted against cycle number.

The average efficiencies for the first 1000 cycles are as follows: ϵ_e, 63.1%; ϵ_v, 79.1%; and ϵ_c, 79.7%.

Late in 1979, another test was conducted to ascertain the stability of the system's voltaic performance by comparing it with the performance of a 1979 single-cell design. Figure 8 compares voltage *vs.* current density data for the two cell systems. The reported cell voltages were obtained using probes directly on the chlorine electrodes in both systems. As measured in this manner, the voltaic performance of the 1.7 kW h cell system was nearly equivalent to that of cells containing 1979 technology. The apparent 1% reduction in the voltaic efficiency of the 1.7 kW h cell system, as measured at the terminals over its first 1000 cycles and reported in Fig. 8, is due to increased contact resistances in the internal bus work and not due to a loss in chlorine-electrode activity. An important measure of the system is the fact that it has consistently delivered an average energy of 1.62 kW h during discharge over the entire 1000 cycles. This performance parameter is illustrated in Fig. 9.
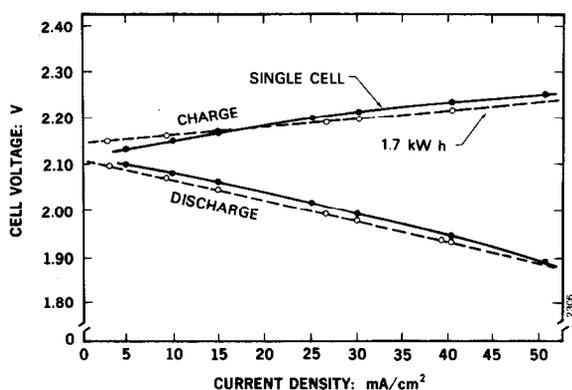
Fig. 8. Voltaic performance comparison of cells in the 1.7 kW h system, utilizing early 1976 technology, and a single-cell incorporating 1979 technology.
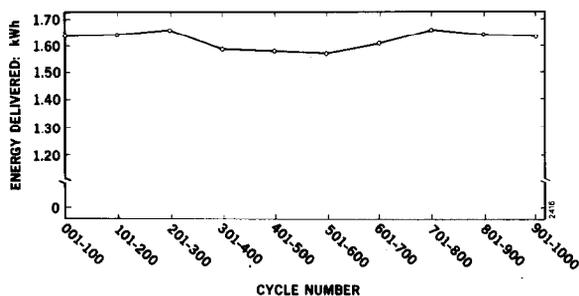
Fig. 9. Delivered energy of the 1.7 kW h cell system as a function of cycle number.

During almost four years of cycling, only one performance degradation mode has been identified in the system. It has occurred six times, and in each case the gas vent holes in some of the chlorine-electrode pairs became plugged with an unknown substance. These occurrences were accompanied by an average decrease in energy efficiency of 3.3%. However, the energy efficiency regained its previous level after removal of the foreign material from the vent holes.

Table 2 shows the results of the elemental analysis performed to determine the composition of this material. All of the elements in Table 2, except fluorine, would be considered normal components in an operational battery system. Based on this fact, it was concluded that the source of the substance was probably one or more of the plastic materials used, since the plastics are the only sources of fluorine in the system.

TABLE 2

Elemental analysis of vent-hole debris

Material	(%)
Carbon	16.5
Hydrogen	0.8
Nitrogen	0.5
Fluorine	6.6
Chlorine	32.0

The two possible sources of fluorine are polyvinylidene fluoride (manufactured under the tradename Kynar), which is used for the stack-sump case as well as for the tube connectors, and polytetrafluoroethylene (tradename Teflon, PTFE), which is used in its ordinary form for tubing and pump gears, and in a specialized form for the top inside seal of the cell case.

During the 1000 cycles logged to date, the electrolyte has been changed 35 times. Categorically, these changes have been made either after mechanical failures or to improve cell system performance. Most of the changes were made due to failures of peripheral components. However, a total of 138 cycles were completed without requiring a change of electrolyte.

Discussion

The 1.7 kW h cell system has attained 40% of the cycle life target for a commercial load-leveling battery, and consequently has demonstrated the stability of the porous graphite–chlorine electrodes. Over one-half year of unattended operation, or 138 cycles without electrolyte maintenance, has been achieved to date. Internal inspection of the cell and examination of electrode voltage data indicate that the chlorine electrodes have remained stable. There is every reason to believe the goal of 2500 cycles will be

reached, that the electrodes will continue to remain active and stable, and that the system will be able to cycle unattended for one full year (250 cycles).

These goals appear even more attainable in light of a recent modification of the 1.7 kW h system to eliminate auxiliary components that have created an excessive maintenance burden without contributing to the purpose of the life test [5]. Figure 10 shows a schematic drawing of the refurbished system. A cursory comparison of this support system with the former peripheral subsystem shown in Fig. 5 reveals that the refurbished support system has much greater simplicity.
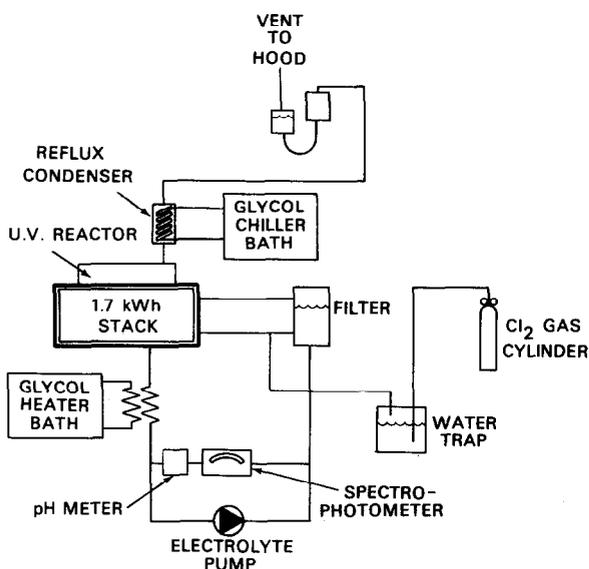
Fig. 10. Schematic of the 1.7 kW h system modified in November 1979 to eliminate failure-prone components not essential to the purpose of life testing of the all-graphite stack.

Acknowledgments

References

1 Energy Development Associates, Development of the zinc–chloride battery for utility applications, Palo Alto, CA: *Electric Power Res. Inst., April 1979, EM-1051*, Part I, Section 1, p. 3.
2 Energy Development Associates, Development of the zinc–chloride battery for utility applications, Palo-Alto, CA: *Electric Power Res. Inst., April 1979, EM-1051*, Part IV, Section 28, pp. 2 - 3.
3 Energy Development Associates, Development of the zinc–chloride battery for utility applications, Palo Alto, CA: *Electric Power Res. Inst., April 1979, EM-1051*, Part IV, Section 25, pp. 4 - 6.
4 Energy Development Associates, Development of the zinc–chloride battery for utility applications, Palo Alto, CA: *Electric Power Res. Inst., May 1980, EM-1417*, Part IV, Section 22, pp. 1 - 8.
5 Energy Development Associates, Development of the zinc–chloride battery for utility applications, Palo Alto, CA: *Electric Power Res. Inst., May 1980. EM-1417*, Part IV, Section 23, pp. 1 - 6.